AUTOMATIC BUILDING ROOF SEGMENTATION BASED ON PFICA ALGORITHM AND MORPHOLOGICAL FILTERING FROM LIDAR POINT CLOUDS

Saman Ghaffarian[1], Salar Ghaffarian[2], Youssef El merabet[3], Zineb Samir[3], Yassine Ruichek[4]
[1]Faculty of Geo-Information Science and Earth Observation (ITC), University of Twente, Enschede 7500 AE, The Netherlands,
Email: s.ghaffarian@utwente.nl
[2]Independent researcher, South Shariati, Kuye Danesh, 10th Danesh, No:99, Tabriz, Iran,
Email: salarghaffarian1363@gmail.com
[3]Laboratoire LASTID, Département de Physique, Faculté des Sciences, Université Ibn Tofail, BP 133, 14000 Kenitra, Morocco,
Emails: y.el-merabet@univ-ibntofail.ac.ma and z.samir@univ-ibntofail.ac.ma
[4]Laboratory IRTES-SeT, University of Technology Belfort-Montbéliard, 13 rue Ernest Thierry-Mieg, 90010 Belfort, France,
Email: yassine.ruichek@utbm.fr

KEY WORDS: Building roof segmentation, LiDAR, Morphological filtering, PFICA, 3D point clouds.

ABSTRACT: In this study, we propose a new approach for segmenting building roofs from Light Detection And Ranging (LiDAR) point clouds. The algorithm takes advantage of height gradients to automatically seed Purposive FastICA (PFICA) algorithm. The PFICA algorithm with a novel seeding method is implemented to detect ridge points from point clouds of building roofs. Then, 2D coordinates are used to rasterize the detected points. Eventually, morphological filtering and thinning algorithms are used to extract inner and external boundaries of the building roofs. In addition, the potential of PFICA algorithm in clustering 3D point clouds are discussed. The results obtained on a set of LiDAR point clouds demonstrate the efficiency of the developed method in automated segmentation of the building roofs with various characteristics.

1. INTRODUCTION

With the development of technology in generating topographic data such as LiDAR (Light Detection and Ranging) that provide 3D geo-spatial information, new methods are needed for segmenting and modeling of the earth surface. Therefore, 3D building modeling as an indispensable component in urban and rural areas has been an active research topic.
LiDAR data provide 3D point clouds, which are not in a grid (pixel) format like images. However, grid format of these data can be driven from point clouds as Digital Elevation Model (DEM) or Digital Surface Model (DSM) while these products are not as accurate as raw LiDAR data. Thus, direct segmentation and modeling of the buildings from the data of laser points is quite necessary.
In extraction of buildings in urban areas from LiDAR point clouds, some methods can be used to filter and separate the point cloud of a building roof from that of the ground. Then, the extracted point clouds correspond to the building roofs are considered individually to be classified as the most important part and first step of 3D building reconstruction. In object-based classification methods, segmentation step is the fundamental process to have an accurate final classification result. Therefore, point clouds of a building roof are classified by using suitable segmentation methods considering geometrical planes in the roof (Yan et al., 2015). Finally, building roof can be constructed based on segmentation and classification (if been needed) results based on geometrical features.
Comprehensive literature reviews about various approaches in this field have been made available in (Vosselman, 1999; Brenner, 2005; Haala and Kada, 2010). In the literature, various 3D point cloud segmentation methods have been developed. The proposed methods are mostly based on signal processing and statistical learning algorithms, which use similarity of points, e.g., heights or normal vectors such as region growing (Rottensteiner, 2003; Dorninger and Pfeifer, 2008), RANdom Sample Consensus (RANSAC) method (Tarsha-Kurdi et al., 2008; Hebel and Stilla, 2012), Hough transformation (Maas and Vosselman, 1999; Alharthy and Bethel, 2002), and clustering methods (Sampath and Shan, 2010; Shi et al., 2011; Kong et al., 2013). Building roof segmentation and reconstruction methods can be categorized into two groups with regard to the use of ridge information; 1- Methods that extract building roof ridges (Sampath and Shan, 2010; Kong et al., 2013; Fan et al., 2014; Yan et al., 2015), 2- Methods that do not extract building roof ridges as a preprocess (Huang et al., 2013; Xiong et al., 2014; Song, 2015). Since our proposed method uses ridge information, we dedicate our literature review to group one studies. For instance, Sampath and Shan (2010) extract breakline points (ridges) by computing the dimensionality of each point using eigenvalues before clustering the point clouds and segmentation of building roof. However, their proposed breakline point extraction method cannot extract all of the breakline points

specially the points on the external boundaries of the buildings. They deduced that non-planar (breakline) points can influence the accuracy of the final segmentation results. Furthermore, they utilized an automated fuzzy K-means algorithm to segment the building roofs after excluding non-planer points. Yan et al. (2015) extracted roof ridges and internal boundaries between adjacent roof facets to generate 2D topology of the building roofs. Then, they used an improved 2D Snake algorithm to segment the building roofs. However, their proposed method is based on several parameters to be predefined. In a different study, Fan et al. (2014) developed a method that starts with detecting roof ridges using RANSAC algorithm. Further, the extracted roof ridges are utilized to indicate the location and direction of the gabled roofs. They showed that their proposed method can segment building roofs with high correctness and completeness ratio. However, their method fails where two roof facets are immediately adjacent to each other and when the point cloud density is not high enough. Kong et al. (2013) used ridge lines to estimate geometrical planes after using Fuzzy K-means and K-plane clustering methods to efficiently segment the building roofs. In addition, they demonstrated that their proposed method can rapidly and appropriately classify the building roofs. Their developed method fails to extract all the ridge lines directly and they are needed to be estimated based on additional rules.

Recently, Independent Component Analysis (ICA) has been studied for remote sensing applications to improve the efficiency of the existing methods or to develop a new model to solve the known quandaries (Bita et al., 2006; Birjandi and Datcu, 2010; Chen et al., 2012). In these studies, efficiency of the ICA-based methods in signal and image processing topics are demonstrated. However, ICA-based methods' performance was not investigated for 3D LiDAR point clouds applications. Besides, ICA algorithm is defined as Blind Source Separation (BSS) method, which limits the use of ICA in object detection and segmentations applications. Purposive FastICA (PFICA) was developed as an improved FastICA algorithm that overcomes the limitations of the FastICA by giving ability to be targeted to extract a specific feature from remote sensing images (Ghaffarian and Ghaffarian, 2014).

In this paper, we present a new approach based on Purposive FastICA (PFICA) algorithm and morphological filtering to automatically segment the building roofs. Our proposed method starts with extracting ridges in building roof using a new PFICA seeding method based on gradients of the height values of the laser points to efficiently detect ridge points from LiDAR point clouds. Then, the detected points are rasterized into 2D image space as a binary image. Finally, morphological filtering and thinning algorithms are used to extract final building roof segmentation results. In addition, potential of the PFICA algorithm in processing (clustering) LiDAR point clouds is demonstrated and discussed.

2. BASICS

2.1. ICA

Independent Component Analysis (ICA) is known as a Blind Source Separation (BSS) technique (Herault and Jutten, 1986). Further, Hyvarinen (1998) assumed signals as sources and implemented ICA as a blind signal separation method. He used ICA to declare a set of random variables as linear combinations of statistically independent component variables. Let $V = (v_1, v_2, \dots, v_k)^T$ as a k-dimensional source signal vector whose components are statistically independent, and $X = (x_1, x_2, \dots, x_n)^T$ as an n-dimensional observed signal vector have a linear combination of independent source signals based on an unknown mixing matrix U as follow:

$$X = UV \tag{1}$$

In this letter, the vector X is known from LiDAR point clouds data. The source vector V is the goal of the ICA algorithm. To compute source vector V from the remotely sensed vector X an unmixing matrix R is utilized as follow:

$$W = RX \tag{2}$$

In the equation above, W is an estimation of source signals, where $W = (w_1, w_2, \dots, w_m)^T$ are as independent as possible and U is the inverse of R.

To achieve best estimation of the source signal V from ICA algorithm three assumptions are considered as follows: 1- Number of estimated components (sources) equals to number of inputs signal vectors X; 2- The components in V are statistically independent; 3- Independency of the components are based on non-Gaussianity.

2.2. FastICA

FastICA algorithm speeds up the ICA algorithm without a major effect on efficiency of the results. FastICA algorithm maximizes non-Gaussianity based on a fixed-point iteration (Hyvärinen, 1999), which can also been computed using Newton iteration method. FastICA starts with centering input vector data Xusing equation below:

$$X = X - E\{X\} \tag{3}$$

Then, in order to uncorrelate the components (with a variation value one) the input vector data $X$is whitened as follow:

$$\gamma = \frac{E^T X}{\sqrt{D}} \tag{4}$$

where $D$is the diagonal matrix of eigenvalues of covariance matrix ($E\{XX^T\}$). $E$is the matrix of eigenvalues. Indeed, the FastICA algorithm maximizes the non-Gaussianity of the projection $R^T\gamma$ for data$X$, and finds the direction from Eq. (4). In this letter, function $g(\alpha)$is used as a non-quadric function to extract independent components as follows:

$$g(\alpha) = \log\cos h(\alpha) \tag{5}$$

$$g'(\alpha) = \tan h(\alpha) \tag{6}$$

$$g''(\alpha) = 1 - \tan h^2(\alpha) \tag{7}$$

where $g'(\alpha)$ and $g''(\alpha)$ are the first and second derivatives of function $g(\alpha)$, respectively.
Then, the unmixing matrix R is iteratively renewed to extract final independent components using equation below:

$$R = E\{\gamma g'(R^T\gamma)\} - E\{g''(R^T\gamma)\}R \tag{8}$$

Each iteration is finalized by computing the normal value of $R$to increase the stability of the algorithm:

$$R = {R}/{\|R\|} \tag{9}$$

The fixed-point iteration is stopped when the changes in the direction of R are very small, which can be predefined as a threshold value.

2.3. PFICA

Purposive FastICA (PFICA) algorithm (Ghaffarian and Ghaffarian, 2014) improves FastICA by adding capability of initializing unmixing matrix R using Moore-Penrose pseudo inverse matrix. Consequently, by seeding the PFICA algorithm final results become stable, and thus, selection of components can be automated with an appropriate initialization.
Let the reference component Z is one estimated component and R_0 is the corresponding column of the unmixing matrix that can be computed as follow:

$$Z = XR_0 \tag{10}$$

where $Z = (z_1, z_2, \dots, z_n)^T$, n is the number of samples. Therefore, R_0as an estimated component can be calculated using equation below:

$$R_0 = X^{\dagger}Z \tag{11}$$

where $X^{\dagger}$ is the Moore-Penrose pseudo inverse of the matrix X. Finally, R_0matrix is utilized as seeding matrix for the FastICA algorithm instead of randomly initializing procedure.

3. THE PROPOSED METHOD

The PFICA algorithm was introduced for automatically detecting buildings from high resolution images. In this case bands of the images are used as input data, and seeding operation is based on statistical relations between pixel values. Then, result is generated by maximizing the non-Gaussianity between pixel values. However, in LiDAR point clouds there are only geometric relations between point clouds, which are not appropriate information for segmenting building roofs. Thus, first step is to compute appropriate information as input data X. To do so, normal vectors for each point are calculated by choosing points using k-nearest neighborhood (K-nn) method (Sankaranarayanan et al., 2007). The k-nearest neighborhood method is specially selected because it allows selecting as many as neighborhood points that are needed in computing normal vectors. The normal vectors are selected as input data for PFICA algorithm. The input data matrix X becomes a three dimensional matrix. In addition, considering the rules to obtain best estimation results from the ICA algorithm, number of estimated components should equals to number of input signals X. Therefore, the PFICA algorithm should be seeded with a three dimensional matrix (data), indeed, three seeding information are needed.

Initially, gradients between the heights of the points are computed for each point for m number of nearest points. The distances between points are calculated based on three dimensional Euclidean equation. For example, if m has a value of three, each point has three gradients for three of nearest points. Then, p numbers of probes are randomly distributed among point clouds. These probes start to evolve toward ridges based on following rules:

1) Find m number of nearest points using three dimensional Euclidean distance.

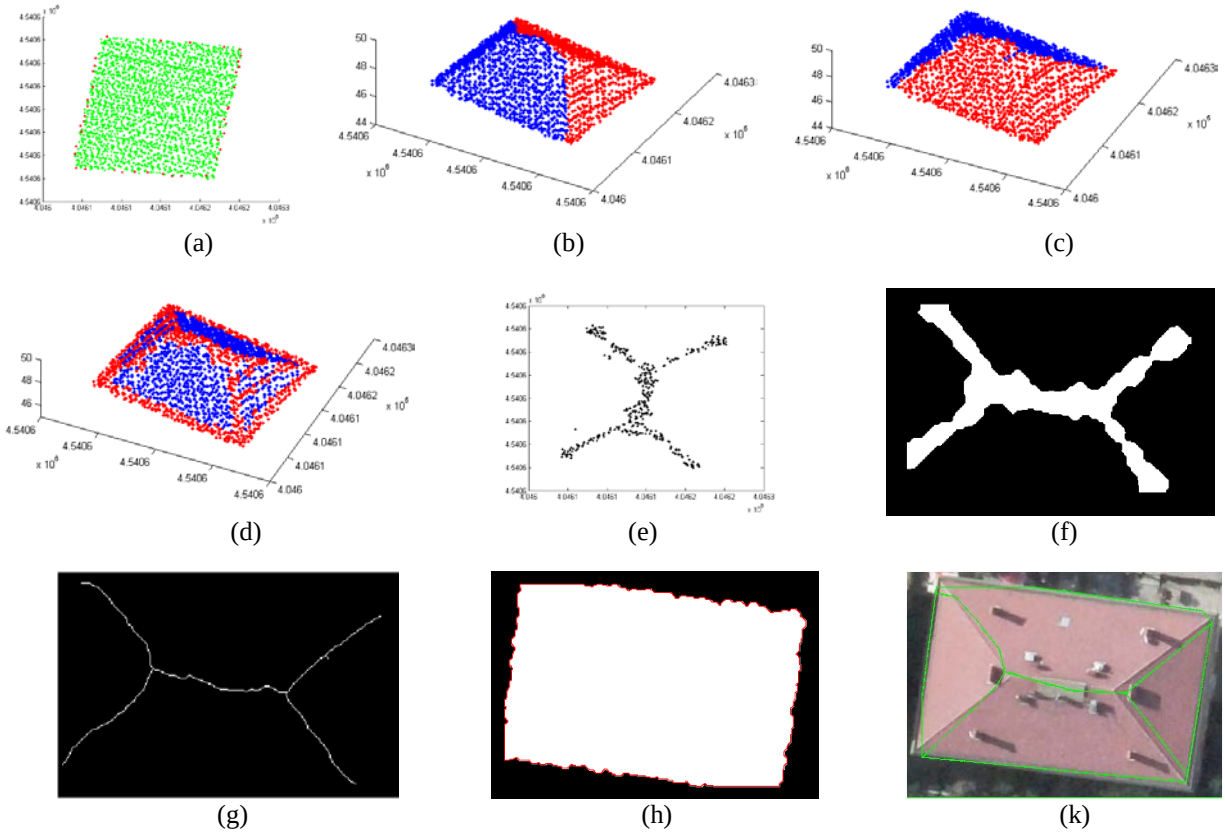

Fig. 1. The illustration of steps of the proposed automatic building roof segmentation method for test building #1. (a) The results for seeding PFICA algorithm, where the red points are the seeding points, (b), (c) and (d) are the results of PFICA algorithm after implementing binary k-means for IC1, IC2 and IC3, respectively, (e) 2-D illustration of the points after refinement as input for inner boundary extraction, (f) morphological filtering result after rasterizing the inner ridge points, (g) Morphological thinning result, (h) external boundary extraction result overlaid on morphological filtering result for external ridge points, (k) final result after merging inner and external segments and executing line simplification algorithm (Douglas-Peucker algorithm).

2) Move to the points that have lowest height among the points which are selected in previous step with no more than a specified threshold value of height gradients. The threshold based on height gradients prevents points from evolving toward noise points.
3) Probe cannot move to the points that previously have crossed that point.

The evolution process stops when there is not a new point which satisfies the above-mentioned rules (Fig. 1a). The detected points are used as first seeding data for PFICA algorithm. Since the detected points denote the ridge points and our goal is to target the PFICA algorithm to detect ridges, the next seeding data are generated randomly from the rest of the point clouds.

After generating the seeding matrix W, the PFICA algorithm is implemented. Since the ridge points are seeded as the first matrix, the IC1 is the component that involves the ridge information. As the final step of PFICA algorithm IC1 is clustered using K-means algorithm with two number of clustering. Then, to remove the remaining points which are not ridge points a method based on eigenvalues is used to find and exclude remaining planer points from remaining points very similar to the method which is used in (Sampath and Shan, 2010). The differences are that in our proposed method k-nn method is used to find points for computing normal of the points and unlike their method we exclude the planer points instead of non-planer points (Fig. 1e). Note that these points are only used for delineating internal ridges, and whole points which are resulted from binary clustering of the IC1 are used for delineating external boundaries (Fig. 1h).

In the final step the points in 2-D space is rasterized using the x and y coordinates of the points. Accordingly, by using the morphological filtering building roofs are segmented. For external boundaries in morphological operations after rasterizing the points, morphological dilation and filling are used and boundary of the object is traced. In addition, for internal boundaries, morphological dilation, opening, closing and thinning algorithms are implemented. As a post process floating internal boundaries are extended to intersect to the external boundaries. Eventually, Douglas-Peucker algorithm (Hershberger and Snoeyink, 1992) is implemented as line simplification method to obtain straight lines.

4. RESULTS AND DISCUSSIONS

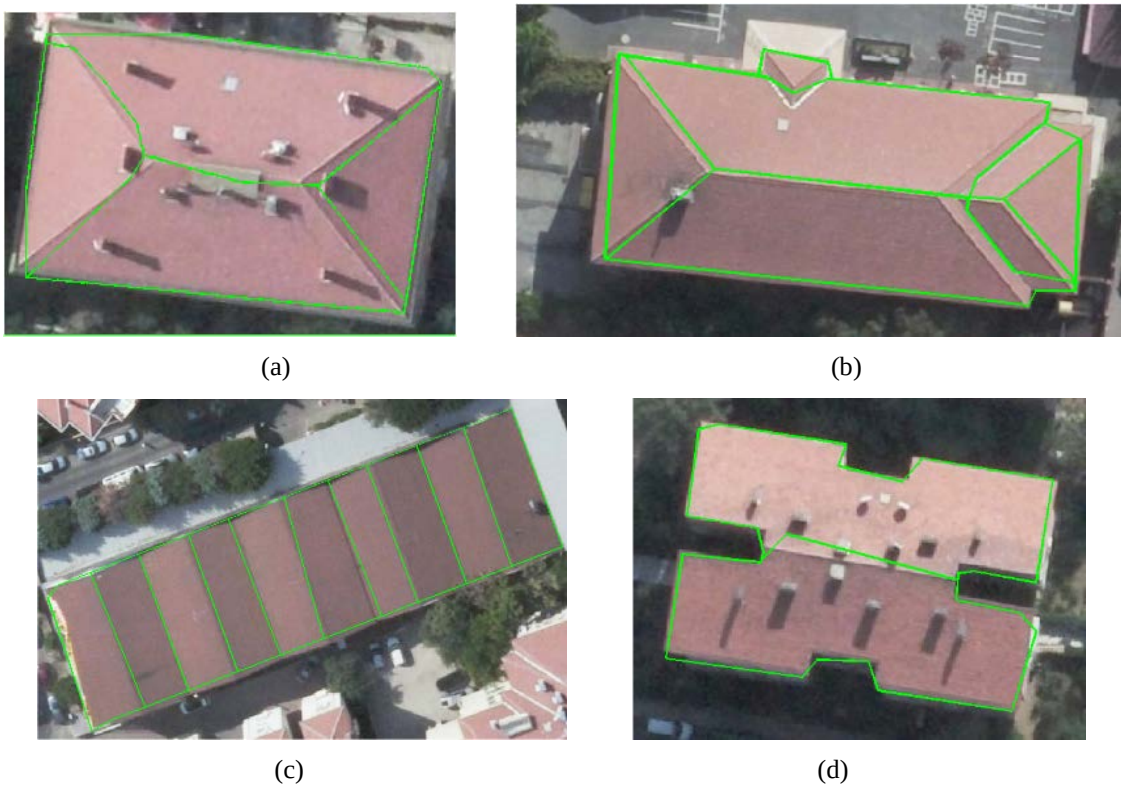

(a) (b)

(c) (d)

Fig. 2. Segmentation results for test buildings #1 (a), #2 (b), #3 (c) and #4 (d) overlaid on very high resolution aerial images.

TABLE I
QUANTITATIVE EVALUATION OF THE PROPOSED METHOD

Building Roof	Number of segmented roof facets	Actual number of roof facets	Completeness (%)
#1	4	4	100
#2	7	11	64
#3	10	10	100
#4	2	2	100
Mean			91

The laser scanning data that is used for the experiments was acquired over Istanbul, Turkey. The data set has an average point spacing of 6 points per m^2. Fig. 2 illustrates the test buildings and the results of our proposed method in segmenting building roofs. These buildings were particularly selected to demonstrate and test the efficiency of the developed method in divers and complicated building roofs segmentation from LiDAR point clouds.

The proposed method is evaluated based on the number of segments that are extracted using our developed method and actual number of segments same as is used by Fan et al. (2014). The results are compared to very high resolution aerial images for qualitative evaluation through visual inspections.

In addition, quantitative results of the developed method are provided considering the number of facets that is segmented by the developed method and the completeness accuracy value for the results are computed (Table I).

Three of four building roofs are segmented with correct number of facets using the proposed method. However, building roof #2 is segmented into 7 number of facets instead of 11 number of facets and produces 64% completeness performance in segmenting building roof from LiDAR point clouds. This low accuracy value is due to proximity of the points around inner ridges. Furthermore, number of points that is used in computing normal vectors is important and influences the results. In this study, 24 nearest number of points are selected using k-nn algorithm to compute normal vector for each point. This value is selected based on the least number of points that PFICA needs to detect ridge point clouds. This number of points in normal vector calculation might lead to miss ridges which are near than selected value. Accordingly,

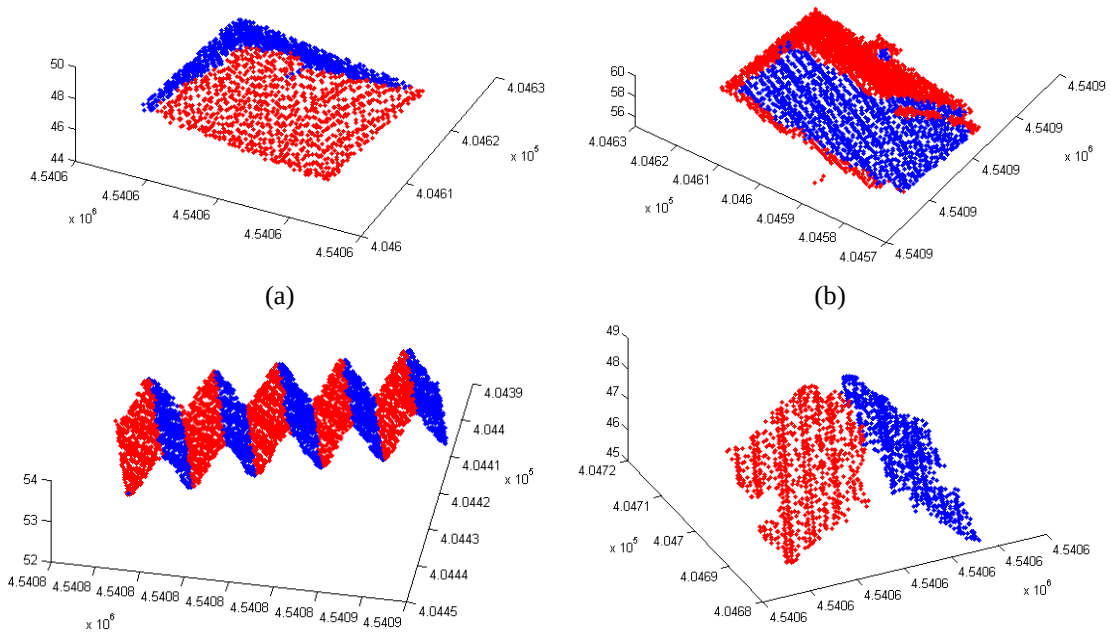

(a) (b) (c) (d)

Fig. 3. Binary k-means clustering of IC2 results for test buildings #1 (a), #2 (b), #3 (c) and #4 (d).

a facet is missed in such a challenging case that point clouds denoting ridges are so close to each other. Furthermore, as it can be seen from Fig. 2b, in upper side of #2 building is a gabled roof which is also detected as one facet instead of two facets due to geometric proximity of the point clouds around ridges. Buildings #1, #3 and #4 are segmented with 100% completeness accuracy values that demonstrate the reliability of the developed method in such cases. In building #3, the building has several connected facets which are detected and segmented correctly not only in terms of number of facets but also in terms of geometrical precision. In buildings #1 and #4 the number of facets is correctly extracted; however, the geometrical precision is low where the ratio of the noise points on the roof of the building is high. Finally, mean completeness accuracy value of 91% is computed for all building roofs, which shows the efficiency of the developed method in automatically segmenting building roofs.

Besides, results of the IC2 after implementing binary k-means clustering for the building roofs are illustrated in Fig. 3 to demonstrate the potential of the PFICA algorithm in clustering point clouds. Since we have three results as independent components which one of them is seeded for detecting ridge points, the other components are seeded randomly. IC2 results for buildings #3 and #4 are quite promising. While IC2 results for buildings #1 and #2 are clustered the most similar point clouds in terms of normal vectors that merges the closest point clouds. However, in right side and upper side of the building roof #2 the small planes are also successfully distinguished from their nearside different planer points. Altogether, as it can be seen from Fig. 3, the PFICA algorithm has the potential of clustering point clouds directly instead of detecting ridge points. The most important challenges in this way are the limited number of resulted ICs and generating appropriate seeding of PFICA algorithm.

5. CONCLUSION

In this letter, we proposed a novel method for automated building roof segmentation using LiDAR point clouds. The method is based on PFICA algorithm with a novel seeding technique and a new approach of morphological filtering. The detected ridge points are rasterized using x and y coordinates of the points to conduct morphological operations. By using gradients of the height data the distributed probes were guided and the PFICA algorithm was seeded and targeted to extract ridge points through building LiDAR point clouds. The new seeding approach leads to detecting ridge points with PFICA algorithm in high accuracy ratio. As it can be seen from Fig. 3 and discussed, the PFICA has the potential of clustering point clouds directly as well as detecting ridge points. However, seeding of PFICA algorithm and limited number of ICs are the remaining problems to be solved. Another limitation of the PFICA algorithm which was observed during this study is that the PFICA algorithm, considering the seeding points, extracts the data which are in larger number. This is also the reason that we used 24 number of points in k-nn for computing normal vectors. However, it leads to merging very close ridge points in the building roofs. Finally, the building roof segmentation results demonstrate the efficiency of the developed method in automatically segmenting building roofs from LiDAR point clouds.

ACKNOWLEDGMENT

The LiDAR data has been provided by Istanbul Metropolitan Municipality.

REFERENCES

Alharthy, A., Bethel, J. 2002. “Heuristic Filtering and 3D Feature Extraction from Lidar Data.” Proceedings of the ISPRS Commission III, Graz, Austria, 9–13.

Birjandi, P., Datcu, M. 2010. “Multiscale and dimensionality behavior of ICA components for satellite image indexing.” IEEE Geosci. Remote Sens. Lett. 7 (1): 103–107.

Bita, I.P.A., Barret, M., Pham, D.A. 2006. “Compression of multicomponent satellite images using independent components analysis.” Indep. Comp. Anal. Blind Signal Separat., Lecture Notes Comput. Sci. 3889: 335–342.

Brenner, C. 2005. “Building reconstruction from images and laser scanning.” Int. J. Appl. Earth Obs. Geoinf. 6: 187–198.

Chen, F., Qin, F., Peng, G., Chen, S. 2012. “Fusion of remote sensing images using improved ICA mergers based on wavelet decomposition.” Proc. Eng. 29: 2938– 2943.

Dorninger, P., Pfeifer, N. 2008. “A comprehensive automated 3D approach for building extraction, reconstruction, and regularization from airborne laser scanning point clouds.” Sensors. 8: 7323–7343.

Fan, H., Yao, W., Fu, Q. 2014. “Segmentation of Sloped Roofs from Airborne LiDAR Point Clouds Using Ridge-Based Hierarchical Decomposition,” Remote Sensing 6: 3284-3301.

Ghaffarian, S., Ghaffarian, S. 2014. “Automatic building detection based on Purposive FastICA (PFICA) algorithm using monocular high resolution Google Earth images,” ISPRS Journal of Photogrammetry and Remote Sensing, 97: 152-159.

Haala, N., Kada, M. 2010. “An update on automatic 3D building reconstruction.” ISPRS J. Photogramm. Remote Sens. 65: 570–580.

Hebel, M., Stilla, U. 2012. “Simultaneous calibration of ALS systems and alignment of multiview LiDAR scans of urban areas.” IEEE Trans. Geosci. Remote Sens. 50: 2364–2379.

Herault, J., Jutten, C. 1986. “Space or time adaptive signal processing by neural network models. Neural Networks for Computing.” AIP Conference Proceedings 151: 207–211.

Hershberger, J., Snoeyink, J. 1992. “Speeding Up the Douglas-Peucker LineSimplification Algorithm.” Technical Report, In Proceedings of 5th International Symposium of Spatial Data Handling: 134-143.

Huang, H., Brenner, C., Sester, M. 2013. “A generative statistical approach to automatic 3D building roof reconstruction from laser scanning data.” ISPRS Journal of photogrammetry and remote sensing 79: 29-43.

Hyvärinen, A. 1998. “Independent component analysis in the presence of gaussian noise by maximizing joint likelihood.” Neurocomputing 22: 49–67.

Hyvärinen, A. 1999. “Fast and robust fixed-point algorithms for independent component analysis.” IEEE Trans. Neural Networks. 10 (3): 626–634.

Kong, D., Xu L., Li, X. 2013. “A new method for building roof segmentation from airborne LiDAR point cloud data.” Meas. Sci. Technol., 24: 1-13.

Maas H., Vosselman, G. 1999. “Two algorithms for extracting building models from raw laser altimetry data.” ISPRS J. Photogramm. Remote Sens., 54(2): 153–163.

Rottensteiner, R. 2003. “Automatic generation of high-quality building models from LiDAR data.” IEEE Comput. Graph. Appl. 23: 42–50.

Sampath A., Shan, J. 2010. “Segmentation and reconstruction of polyhedral building roofs from aerial LIDAR point clouds.” IEEE Trans. Geosci. Remote Sens. 48 (3): 1554–1567.

Sankaranarayanan, J., Samet H., Varshney, A. 2007. “A fast all nearest neighbor algorithm for applications involving large point-clouds.” Comput. Graph 31: 157–74.

Shi, B., Liang, J., Liu, Q. 2011. “Adaptive simplification of point cloud using k-means clustering.” Comput. Aided Des. 43: 910–22.

Song, J., Wu, J., Jiang, Y. 2015. “Extraction and reconstruction of curved surface buildings by contour clustering using airborne LiDAR data.” Optik - International Journal for Light and Electron Optics 126 (5): 513-521.

Tarsha-Kurdi, F., Landes, T., Grussenmeyer, P. 2008. “Extended RANSAC algorithm for automatic detection of building roof planes from LiDAR data.” Photogramm. J. Finl. 21: 97–109.

Vosselman, G. 1999. “Building reconstruction using planar faces in very high density height data.” Int. Arch. Photogramm. Remote Sens. 32: 87–92.

Xiong, B., Oude Elberink, S., Vosselman, G. 2014. “Building modeling from noisy photogrammetric point clouds.” ISPRS Ann. Photogramm. Remote Sens. Spatial Inf. Sci. commission II-3: 197–204.

Yan, J., Zhang, K., Zhang, C., Chen S., and Narasimhan, G. 2015. “Automatic Construction of 3-D Building Model From Airborne LIDAR Data Through 2-D Snake Algorithm.” IEEE Transactions on Geoscience and Remote Sensing 53 (1): 3-14.